

Thermodynamic behavior of the XXZ Heisenberg $s = 1/2$ chain around the factorizing magnetic field

This article has been downloaded from IOPscience. Please scroll down to see the full text article.

2010 J. Phys.: Condens. Matter 22 216008

(<http://iopscience.iop.org/0953-8984/22/21/216008>)

View [the table of contents for this issue](#), or go to the [journal homepage](#) for more

Download details:

IP Address: 129.252.86.83

The article was downloaded on 30/05/2010 at 08:12

Please note that [terms and conditions apply](#).

Thermodynamic behavior of the XXZ Heisenberg $s = 1/2$ chain around the factorizing magnetic field

J Abouie^{1,2}, A Langari³ and M Siahatgar³

¹ Department of Physics, Shahrood University of Technology, Shahrood 36199-95161, Iran

² School of Physics, Institute for Research in Fundamental Sciences (IPM), Tehran 19395-5531, Iran

³ Department of Physics, Sharif University of Technology, Tehran 11155-9161, Iran

E-mail: jahan@shahroodut.ac.ir

Received 21 March 2010, in final form 14 April 2010

Published 5 May 2010

Online at stacks.iop.org/JPhysCM/22/216008

Abstract

We have investigated the zero- and finite-temperature behaviors of the anisotropic antiferromagnetic Heisenberg XXZ spin-1/2 chain in the presence of a transverse magnetic field (h). The attention is concentrated on an interval of magnetic field between the factorizing field (h_f) and the critical one (h_c). The model presents a spin-flop phase for $0 < h < h_f$ with an energy scale which is defined by the long range antiferromagnetic order while it undergoes an entanglement phase transition at $h = h_f$. The entanglement estimators clearly show that the entanglement is lost exactly at $h = h_f$, which justifies different quantum correlations on both sides of the factorizing field. As a consequence of zero entanglement (at $h = h_f$) the ground state is known exactly as a product of single-particle states which is the starting point for initiating a spin wave theory. The linear spin wave theory is implemented to obtain the specific heat and thermal entanglement of the model in the interested region. A double-peak structure is found in the specific heat around $h = h_f$, which manifests the existence of two energy scales in the system as a result of two competing orders before the critical point. These results are confirmed by the low temperature Lanczos data which we have computed.

(Some figures in this article are in colour only in the electronic version)

1. Introduction

The zero-temperature phase diagram (i.e. quantum phase diagram) of a model gives important information on the low temperature behavior of the system [1, 2]. The anisotropic antiferromagnetic Heisenberg (XXZ) spin-1/2 model shows different quantum phases with respect to a symmetry breaking transverse field (non-commuting magnetic field) [3–5]. The non-commuting field imposes quantum fluctuations into the ground state which can induce new phases. Cs_2CoCl_4 is a quasi-one-dimensional spin-1/2 XY -like antiferromagnet with weak inter-chain couplings ($J'/J = 0.014$) which can be studied in terms of a XXZ chain with anisotropy parameter $\Delta = 0.25$ [6, 7]. The scaling behavior and quantum phase diagram of the XXZ model in the presence of a transverse magnetic field (h^x) have been investigated [3–5, 8].

Recently, the quantum spin models have received a great deal of attention from the quantum information point of view. These are prototype models to implement and examine the idea of quantum computations which require the quantum correlations measured by entanglement. Hence, disentangled ground states have to be avoided for such implementations. On the other hand, the zero-entanglement property of a ground state provides an exact form for it in terms of the product of single-particle states. The investigation in this direction resumed recently following the seminal work of Kurmann *et al* [9]. Several efforts have been devoted to this direction which is important for condensed matter researchers, i.e. finding an exact (factorized) ground state even at particular values of the coupling constants [10–13]. The factorized (exact) ground state is an accurate starting point to investigate the quantum nature of a phase close to the factorizing point in

addition to some exact knowledge which gives the factorized point. This property is implemented in this paper to initiate a spin wave theory to describe the thermodynamic properties of the XXZ model in the presence of a transverse magnetic field.

The $U(1)$ symmetry of the XXZ model is lost upon adding the transverse magnetic field. Initially, a perpendicular antiferromagnetic order is stabilized by promoting a spin-flop phase (which has a partial moment projection along the field direction). At the factorizing field (h_f) in the spin-flop phase the ground state is known exactly as a direct product of single spin states and the staggered magnetization along the y direction is close to its maximum value. In our model the factorizing field is $h_f = J\sqrt{2(1+\Delta)}$, where quantum fluctuations are uncorrelated and the ground state is the classical one (J is the scale of energy and Δ is the anisotropy parameter). For slightly larger magnetic field very close to the critical one ($h_f < h < h_c$) the antiferromagnetic order becomes unstable and the staggered magnetization falls rapidly to vanish at the critical point. For $h > h_c$ the spins become aligned in the x direction and a fully polarized phase will appear. The region between the factorizing and the critical fields ($h_f < h < h_c$) is the main issue of our study which is not well understood so far.

The zero-temperature properties of the intermediate region ($h_f < h < h_c$) induces its signature into the thermodynamic functions of the model. We have found that this region is characterized by two energy scales and its fingerprint will appear as a double peak in the specific heat. Moreover, the existence of more than an energy scale in the model can be related to a spontaneous symmetry breaking (SSB) [10]. Each broken phase is described by an order parameter which can be zero in the disordered phase. For the aforementioned model the symmetry breaking occurs where the staggered magnetization becomes zero.

The thermodynamic properties of the spin-1/2 XXZ chain in a transverse magnetic field have been studied using the low temperature Lanczos method [15]. However, in this paper we will focus on the intermediate values of h and, more precisely, on the region where a double peak appears in the specific heat of the model. We implement the exact factorized ground state at $h = h_f$ (where the entanglement vanishes) to build up a spin wave theory appropriate to describe the model in intermediate values of the magnetic field. In the linear spin wave approximation we calculate the specific heat and thermal entanglement of the model. Moreover, the spin wave theory gives two different types of quasi-particles which are representing the two energy scales. We have also studied both the zero- and finite-temperature properties of the model on a finite chain using the low temperature Lanczos method [14]. Our numerical results are in agreement with the spin wave theory counterparts. In section 2, we will briefly review the zero-temperature properties of the model from the quantum information point of view. We will provide the spin wave theory in section 3 where the quantum property, specific heat and thermal entanglement are obtained. Finally, the numerical Lanczos results will be presented in addition to discussions on the mentioned topics.

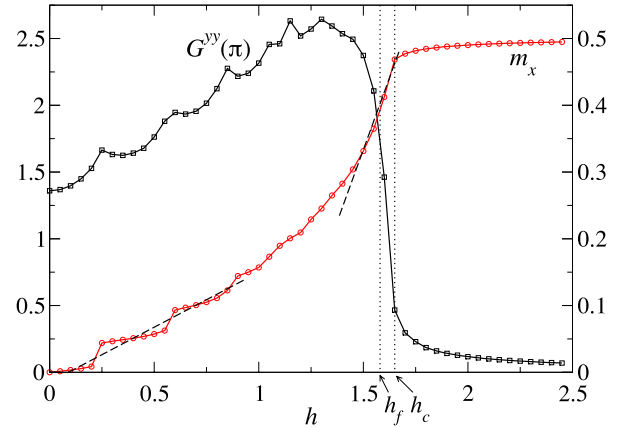


Figure 1. Results of numerical zero-temperature Lanczos method for the magnetization along the x direction (right vertical axis) and the y component spin structure factor at momentum π (left vertical axis) versus the transverse magnetic field h for a chain with $N = 20$ and $\Delta = 0.25$. The magnetization in the z direction is zero.

2. Zero-temperature phase diagram

The anisotropic spin-1/2 Heisenberg model in the presence of a transverse magnetic field is described by the following Hamiltonian:

$$H = J \sum_i (S_i^x S_{i+1}^x + S_i^y S_{i+1}^y + \Delta S_i^z S_{i+1}^z + h S_i^x), \quad (1)$$

where S_i^α s are spin-1/2 operators, Δ is the anisotropy parameter, h is proportional to the transverse magnetic field and the exchange antiferromagnetic coupling J which defines the scale of energy is set to 1. This model has several quantum phases with respect to the transverse magnetic field and anisotropy parameter (Δ). The α -component spin structure factor at momentum p is defined by

$$G^{\alpha\alpha}(p) = \sum_{x=1}^N \langle S_1^\alpha S_{1+x}^\alpha \rangle e^{ipx}, \quad (2)$$

and its increasing behavior in term of system size shows the magnetic order at the specified momentum. We have plotted in figure 1 the magnetization along the x direction ($M_x = (1/N) \sum \langle S_i^x \rangle$) and the y component of the spin structure factor at momentum $p = \pi$ versus h . The value of $\Delta = 0.25$ has been fixed to fit the case of real material Cs_2CoCl_4 . The numerical data has been obtained by the zero-temperature Lanczos method on a finite chain of length $N = 20$ with periodic boundary condition.

The magnetization curve can be distinguished by three parts: (1) magnetization for $0 < h < h_f$, (2) magnetization for $h_f < h < h_c$ and (3) the paramagnetic phase for $h > h_c$. At zero magnetic field, there is no order in the system and all order parameters are zero, i.e. $M_{x,y,z} = 0$. The nonzero value of h starts to align the spins in the x direction and induces a small ferromagnetic order in the x direction. The magnetization, M_x , increases monotonically by increasing the magnetic field. For $h < h_f$ the quantum effects are considerable and the magnetization changes parabolically versus h . Increasing h

suppresses the quantum correlations and they go to zero around h_f . For $h_f < h < h_c$, the magnetization is increased linearly versus h . Magnetization increases up to the critical point (h_c) and saturates at infinite field. Although the staggered magnetization along the y direction becomes zero at the finite critical field, the magnetization in the x direction will be fully saturated only for the isotropic case ($\Delta = 1$) [13]. In other words, the full saturation in the x direction for $\Delta \neq 1$ will happen for $h \rightarrow \infty$. For $h > h_c$ all of the spins align almost completely (for $\Delta \neq 1$) in the x direction and we have a fully polarized paramagnetic phase.

We would like to draw your attention to the region $h_f < h < h_c$, where the model behaves surprisingly. Let us first study the spin chain through the entanglement (τ_2) of two spins [16, 17] which have no classical counterpart. The entanglement is defined by the following relation:

$$\tau_2 = \sum_{i \neq j} C_{ij}^2 \quad (3)$$

where C_{ij} is the concurrence [18] which is implemented instead of the pairwise zero-temperature entanglement between two spins at sites i and j . For the XXZ model, M_z is zero and thus the concurrence takes the form [17], $C_{ij} = 2 \max\{0, C_{ij}^{(1)}, C_{ij}^{(2)}\}$, where

$$C_{ij}^{(1)} = \langle S_i^x S_j^x \rangle + |\langle S_i^y S_j^y \rangle - \langle S_i^z S_j^z \rangle| - \frac{1}{4}, \quad (4)$$

$$C_{ij}^{(2)} = |\langle S_i^y S_j^y \rangle + \langle S_i^z S_j^z \rangle| - \sqrt{\left(\frac{1}{4} + \langle S_i^x S_j^x \rangle\right)^2 - (M^x)^2}.$$

Using quantum Monte Carlo simulation, Roskilde *et al* [10] have shown that, unlike the standard magnetic order parameters (figure 1), the pairwise entanglement plays an essential role at the factorizing field. At the factorizing field (also called the classical field, $h_{cl} = h_f = \sqrt{2(1 + \Delta)}$) [9] the ground state takes a product form [9, 13] and its entanglement is zero. In figure 2, we have plotted $C_{i,i+1}^{(1)}$ and $C_{i,i+1}^{(2)}$ versus the transverse field h for a XXZ spin-1/2 chain with $\Delta = 0.25$ by using the exact diagonalization Lanczos method. At the classical field ($h = h_f \simeq 1.58$), $C_{i,i+1}^{(1)} = C_{i,i+1}^{(2)} = C_{i,i+1}^{(1)} = C_{i,i+1}^{(2)} = 0$. At this point the ground state of the model is factorized (disentangled) where the Néel order is roughly maximized in the y direction.

Let us describe the behaviors of $C_{ij}^{(1)}$ and $C_{ij}^{(2)}$ from a spontaneous symmetry breaking (SSB) point of view. It is found in [10] that the competition between the two functions $C_{ij}^{(1)}$ and $C_{ij}^{(2)}$ demonstrates the appearance of an SSB. In other words, for our model, an SSB can be occurred when $C_{ij}^{(2)} < C_{ij}^{(1)}$. At this condition the magnetic field is greater than the factorizing value ($h > h_f$). Moreover, SSB is usually recognized to happen at the position where the order parameter becomes zero. In our model two standard order parameters, M_x and SM_y (staggered magnetization along the y direction), can represent the quantum phases of the model. We have plotted in figure 1 the magnetization along the x direction (M_x) and the y component of the spin structure factor (G^{yy}) at momentum π for a $\Delta = 0.25$ XXZ spin-1/2 chain. M_x is nonzero in the whole range of magnetic fields: however, $G^{yy}(\pi)$ which is used to show the antiferromagnetic order of the system has

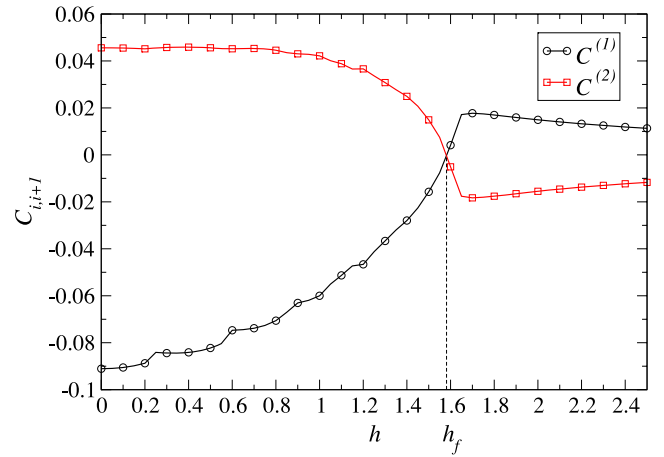


Figure 2. Entanglement estimators of the XXZ spin-1/2 chain versus transverse field h with parameter $\Delta = 0.25$. $C^{(1)}$ is depicted by (black) circles and $C^{(2)}$ by (red) squares. At the classical field ($h = h_f \simeq 1.58$), $C_{i,i+1}^{(1)} = C_{i,i+1}^{(2)} = 0$.

a different behavior. As is observed from our Lanczos data, $G^{yy}(\pi)$ increases by h up to h_f . This behavior is also found in the SM_y curve which has been obtained by the density matrix renormalization group (DMRG) [8]. Thus, no SSB occurs for $h < h_f$. By increasing the magnetic field for $h > h_f$, $G^{yy}(\pi)$ (or equivalently SM_y) decreases rapidly and falls to zero at the critical point h_c . In this respect, a symmetry breaking can occur only for $h > h_f$. In this region, as mentioned before the slope of M_x with respect to h is different from the corresponding one for $h < h_f$.

3. Spin wave theory

As discussed in section 2 the entanglement is zero at the factorizing field (h_f). It allows us to write the many-body ground state as the direct product of the single spin states on odd and even sublattices [9]:

$$|\text{GS}\rangle = \bigotimes_{i \in \text{odd}, j \in \text{even}} |S_i\rangle |S_j\rangle. \quad (5)$$

The spin state on each sublattice is expressed in terms of polar angles (θ, ϕ) which defines the rotation of the up-spin eigenstate of S^z to the specific direction defined by the factorized state. Let us label the odd (even) sublattice by A (B). Thus, (θ, ϕ) represents the A sublattice while (β, α) is the corresponding one for the B sublattice. It has been shown [13] that one can consider $\phi = 0 = \alpha$ without loss of generality. Moreover, the magnitude of the remaining polar angles are equal $|\theta| = |\beta|$ in the case of a homogeneous spin model (like here) and is given by

$$\cos(\theta) = -\sqrt{\frac{1 + \Delta}{2}}. \quad (6)$$

For the antiferromagnetic model the factorized ground state is defined by $\beta = -\theta$.

Before starting the spin wave approach we implement a unitary transformation on the Hamiltonian. All spins on the A

sublattice are rotated by an angle θ counterclockwise around the y direction and clockwise for spins on the B sublattice. The rotated Hamiltonian (\tilde{H}) is the result of rotations on all lattice points, $\tilde{H} = \tilde{D}^\dagger H \tilde{D}$ and $\tilde{D} = \bigotimes_{i \in A, j \in B} \mathcal{D}_i(-\theta) \mathcal{D}_j(\theta)$. The single spin rotation operator is $\mathcal{D}_i(\theta) = \exp(-i\theta S_i^y / \hbar)$. In the rotated spin model, the Hamiltonian will have a factorized ground state which is a ferromagnet at the factorizing field. The rotated spin Hamiltonian is written in terms of boson operators a, b with the following Holstein–Primakoff transformation:

$$\begin{aligned} \tilde{S}_{Ai}^+ &= (2S - a_i^\dagger a_i)^{1/2} a_i, & \tilde{S}_{Ai}^x &= S - a_i^\dagger a_i, \\ \tilde{S}_{Bj}^+ &= (2S - b_j^\dagger b_j)^{1/2} b_j, & \tilde{S}_{Bj}^x &= S - b_j^\dagger b_j, \end{aligned}$$

where $\tilde{S}_{A(B)} = \mathcal{D}_{A(B)}^\dagger S_{A(B)} \mathcal{D}_{A(B)}$ are the rotated spin operators and $\mathcal{D}_{A(B)}$ is the unitary single spin rotation operator. The bosonic Hamiltonian in the linear spin wave approximation, i.e. $\tilde{S}_{Ai}^+ \simeq \sqrt{2S} a_i$; $\tilde{S}_{Bi}^+ \simeq \sqrt{2S} b_i$, is given by

$$\begin{aligned} \tilde{\mathcal{H}} &= N \left[\frac{\Delta}{2} + \frac{h}{h_f} (1 + \Delta) \right] + \sum_{l=0}^N \left(\left[\frac{h}{h_f} (1 + \Delta) - \Delta \right] \right. \\ &\quad \times (a_l^\dagger a_l + b_l^\dagger b_l) - \frac{\Delta}{2} [a_l (b_l^\dagger + b_{l+1}^\dagger) + \text{h.c.}] \\ &\quad \left. + \frac{1}{2} \left(\frac{h}{h_f} - 1 \right) \sqrt{1 - \Delta^2} (a_l + b_l + \text{h.c.}) \right). \end{aligned} \quad (7)$$

To diagonalize the bosonic model we first implement the Fourier transformation and then apply a rotation to the boson operators (a_k, b_k):

$$\begin{aligned} a_l &= \frac{1}{\sqrt{N}} \sum_k e^{-ikl} a_k, & b_l &= \frac{1}{\sqrt{N}} \sum_k e^{-i(kl + \frac{k}{2})} b_k, \\ \psi_k &= \cos \eta_k a_k - \sin \eta_k b_k, & \chi_k &= \sin \eta_k a_k + \cos \eta_k b_k. \end{aligned} \quad (8)$$

The diagonalized Hamiltonian in terms of two sets of quasi-particle operators is given by

$$\tilde{\mathcal{H}} = E_0 + \sum_k (\omega_k^+ \chi_k^\dagger \chi_k + \omega_k^- \psi_k^\dagger \psi_k), \quad (9)$$

where the excitation spectra have the following forms:

$$\begin{aligned} \omega_k^\pm &= \frac{h}{h_f} (1 + \Delta) - \Delta \pm \Delta \cos \frac{k}{2}, \\ E_0 &= \frac{N}{2} (\Delta - h h_f) + \omega_0^+ (t^+)^2 + \sqrt{2N(1 - \Delta^2)} \left(\frac{h}{h_f} - 1 \right) t^+, \\ t^+ &= \frac{\sqrt{\frac{N}{2}(1 - \Delta^2)} \left(1 - \frac{h}{h_f}\right)}{\omega_0^+}. \end{aligned} \quad (10)$$

In the above calculations, a translation $\chi_0 \rightarrow \chi_0 + t^+$ has been performed in the diagonalization procedure of the Hamiltonian (7).

The Hamiltonian is now represented in terms of two quasi-particles (bosons), each defining an energy scale. The two energy scales, which are the excitation energies of each boson, lead to two different dynamics for the system. The consequence of two types of dynamics will be seen in the structure of specific heat which will be studied. However, the existence of two different quasi-particle energies ($\omega_k^+ \neq \omega_k^-$) is the first sign of two dynamics in the model.

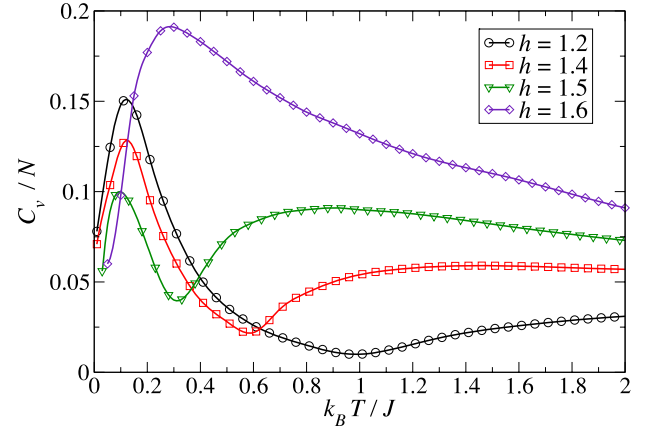


Figure 3. The spin wave results for specific heat of the XXZ model versus T for different values of the transverse magnetic field h and anisotropy parameter $\Delta = 0.25$. (Black) circle is for $h = 1.2$, (red) square: $h = 1.4$, (green) gradient: $h = 1.5$ and (blue) diamond: $h = 1.6$. A narrow peak at low temperature followed by a broader one for higher temperature are observed for $h = 1.4$ and 1.5 .

3.1. Specific heat

To get the finite-temperature properties of the model, we assume $\tilde{n}_k^\pm = \sum_{n^-, n^+} n_k^\pm P_k(n^+, n^-)$, for the spin wave distribution functions, where $P_k(n^+, n^-)$ is the probability of parallel ($n_k^+ = \chi_k^\dagger \chi_k$) and perpendicular ($n_k^- = \psi_k^\dagger \psi_k$) normal modes appearing in the k -momentum state which satisfies $\sum_{n^+, n^-} P_k(n^+, n^-) = 1$ for all ks . The substitutions of $\tilde{n}_k^+ = \langle \chi_k^\dagger \chi_k \rangle$ and $\tilde{n}_k^- = \langle \psi_k^\dagger \psi_k \rangle$ (where $\langle \dots \rangle$ represents the thermal average) in the spin wave Hamiltonian (9) gives the free energy:

$$\begin{aligned} F &= E_0 + \sum_k (\omega_k^+ \tilde{n}_k^+ + \omega_k^- \tilde{n}_k^-) \\ &\quad + T \sum_k \sum_{n^+, n^-} P_k(n^+, n^-) \ln P_k(n^+, n^-). \end{aligned}$$

The number of bosons is controlled by the following constraint which is the magnetization in the x direction:

$$M_x = s - \frac{1}{2N} \sum_k (\tilde{n}_k^+ + \tilde{n}_k^-) - \frac{(t^+)^2}{2N}. \quad (11)$$

The free energy is minimized with respect to $P_k(n^+, n^-)$ s under the constraint of (11) which is applied by a Lagrange multiplier (μ) via the boson's occupation number:

$$\tilde{n}_k^\pm = \frac{1}{e^{\frac{1}{h_f T} (\omega_k^\pm - \mu)} - 1}. \quad (12)$$

The constraint (11) is applied by the values of $M_x(h, T)$ which have been obtained by the numerical Lanczos method. We have plotted in figure 3 the specific heat of the $\Delta = 0.25$ XXZ spin-1/2 chain versus temperature and different values of magnetic field. A double peak is observed in the specific heat which is the signature of the existence of two comparable energy scales. More precisely, the specific heat for $h = 1.4$ and 1.5 has a narrow peak at low temperature ($T \simeq 0.2$) and a broader one at higher T . We will discuss more on this point in section 3.2.

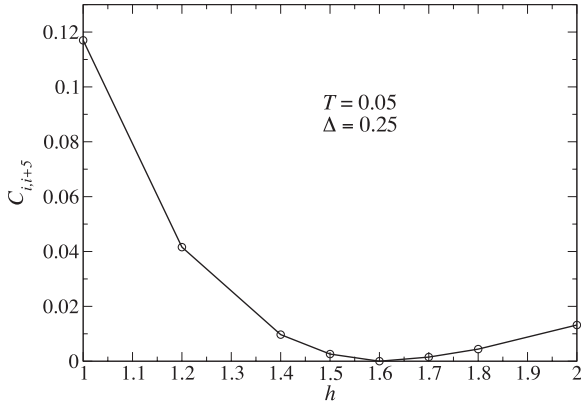


Figure 4. Thermal entanglement of the XXZ model versus h and anisotropy parameter $\Delta = 0.25$ at $T = 0.05$ which has been obtained by the spin wave approximation. Because of the tiny contribution of excited states to the entanglement, its value at h_f is $\sim 10^{-3}$.

3.2. Thermal entanglement

The established spin wave theory close to the factorizing point is used to obtain the thermal behaviors of the correlation functions in equations (4) and consequently to calculate the concurrence. This method can describe the thermal entanglement of two spins in the linear spin wave approximation. In this approach, one can find the following expression for $C_{ij}^{(1)}$ and $C_{ij}^{(2)}$:

$$C_{ij}^{(1)} \simeq -\frac{1}{2N} \left(\sum_k (\tilde{n}_k^+ + \tilde{n}_k^-) + (t^+)^2 \right),$$

$$C_{ij}^{(2)} \simeq \frac{1}{2N} \left(\sum_k \text{Cos}(k \cdot r + k/2) (\tilde{n}_k^+ - \tilde{n}_k^-) + (t^+)^2 \right).$$

As is seen from these functions, $C_{ij}^{(1)}$ is always less than zero, thus the concurrence is $2 \max\{0, C_{ij}^{(2)}\}$. We have plotted in figure 4 the thermal entanglement of the $\Delta = 0.25$ XXZ spin-1/2 chain versus transverse field at temperature $T = 0.05$. By increasing the magnetic field, quantum fluctuations are decreased and the thermal entanglement is declined. At the factorizing point, quantum fluctuations become approximately uncorrelated and the thermal entanglement is very close to zero ($\sim 10^{-3}$). It means that the thermal entanglement is mainly originated from the ground state and the excited states have a very tiny contribution to the entanglement.

4. Summary, discussions and Lanczos results

We have studied the effects of a transverse magnetic field on the zero- and finite-temperature properties of a $\Delta = 0.25$ XXZ spin-1/2 chain. We have focused our attention on the intermediate region of $h_f < h < h_c$ where the model behaves more interestingly.

Kenzelmann *et al* [6] have investigated experimentally the effects of a transverse magnetic field on the quasi-one-dimensional spin-1/2 antiferromagnet Cs_2CoCl_4 , using single-crystal neutron diffraction. Due to the weak inter-chain couplings in Cs_2CoCl_4 ($J'/J = 0.014$) [7], where J is

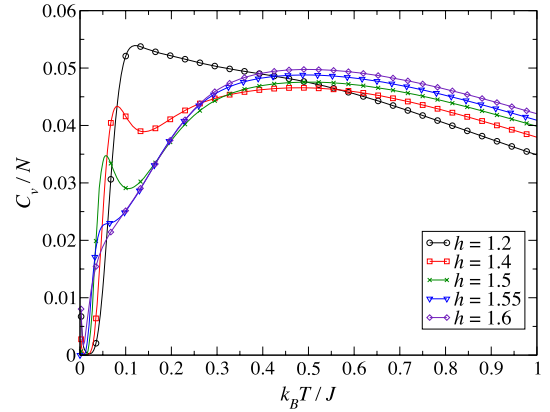


Figure 5. The numerical Lanczos results for the specific heat of XXZ model versus T for different values of transverse magnetic field and $\Delta = 0.25$. At the intermediate region of h , a double-peak structure is observed which indicates the existence of two energy scales in the system.

the coupling within a chain, it is proposed in [6] that the bulk material has a spin liquid phase at the interval $h_f < h < h_c$. In a spin liquid phase all order parameters should be zero and there should be no long range order in the system. The existence of very weak coupling between magnetic chains in this material makes it feasible to be described by a one-dimensional spin-1/2 XXZ model with the anisotropy parameter $\Delta = 0.25$. However, for the 1D XXZ model in the region $h_f < h < h_c$ both magnetization and staggered magnetization are nonzero. Thus the ground state of the model could not be a spin liquid phase. Although the behaviors of the magnetic orders for this region are clearly known, the lacuna of a perfect study of the properties of the system at the intermediate region is still felt. In this respect, we have devoted our attentions to surveying the magnetic and thermodynamic behavior of the system at the intermediate region of the transverse field.

We have implemented the low temperature Lanczos method (LTLM) [14, 15] to compute the thermodynamic behaviors of the model for a chain of finite length. LTLM has been used since it is accurate for low temperatures and especially the thermodynamic averages reach the ground state expectation values as temperature approaches zero. The specific heat versus temperature for different values of the magnetic field on a chain of $N = 20$ and with $\Delta = 0.25$ has been plotted in figure 5. The sampling is taken over $R = 100$ Lanczos numerical data, which have been obtained by different initial random states. The finite size effect can be ignored since the number of sampling (R) is rather high. The result of the spin wave theory (figure 3) and LTLM (figure 5) are in mutual agreement; moreover, both figures show the presence of a double peak in the specific heat for $h = 1.4$ and 1.5 which is evidence for the existence of two scales of energy, or equivalently two dynamics in the system.

The specific heat versus T for all values of the magnetic fields has a Schottky-like peak at low temperatures which is a remarkable feature of the antiferromagnetic behavior. For small values of the magnetic field ($h < 1.4$) the Schottky

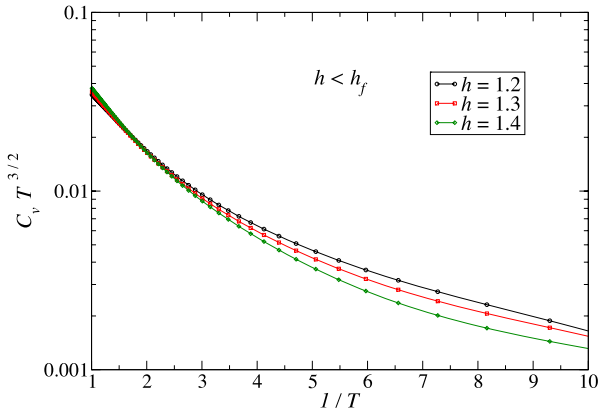


Figure 6. $c_v T^{3/2}$ of XXZ model versus $1/T$ for different values of $h < h_f$ and $\Delta = 0.25$. At low temperatures the slope of the curve shows increasing energy gap in the system.

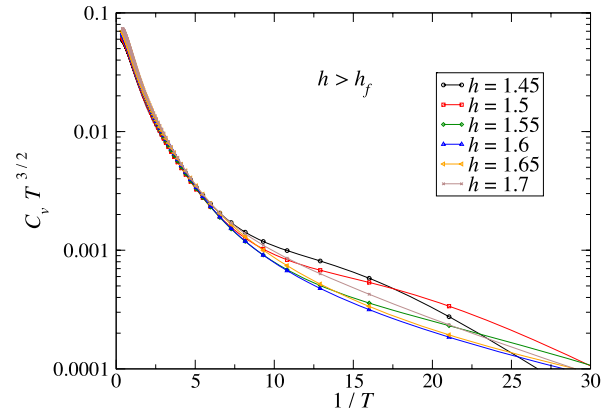


Figure 7. $c_v T^{3/2}$ of XXZ model versus $1/T$ for different values of $h > h_f$ and $\Delta = 0.25$. At low temperatures, the slope of the curve is decreased from $h = 1.45$ to 1.6 and then starts to increase by increasing h .

anomaly is the only one which justifies the existence of a single dynamics in the model. Further increasing the magnetic field (being close to the factorizing point) a broader peak emerges in the specific heat data versus T . This bump is the result of the paramagnetic order. Two different orders are in competition and its signature is especially observable for magnetic fields in the region $h_f \lesssim h < h_c$, where the magnitude of the two types of ordering becomes comparable. The antiferromagnetic order in the y direction is the result of exchange coupling in the broken $U(1)$ symmetry phase. The effect of transverse magnetic field as a paramagnetic order in the x direction shows its presence when it is large enough to define a new scale of energy. Around the factorizing field the two orders manifest their influence on the model as a narrow and broader peak of the specific heat which happens for $h_f \lesssim h < h_c$. This is the region where the spontaneous symmetry breaking is starting to happen. At the critical point (h_c) the antiferromagnetic order vanishes and the paramagnetic order is the only representative of the model. A broader peak in the specific heat versus T is significant for $h > h_c$, which justifies the paramagnetic order.

Employing the specific heat data, one can also scan the behavior of the energy gap (E_g). The existence of an energy gap in the model is clearly observed by the exponential decay of the specific heat at very low temperatures ($T \lesssim 0.02$).

At enough low temperatures ($T < E_g$) the specific heat and energy gap are related by [7]

$$c_v T^{3/2} \propto e^{-\frac{E_g}{T}}. \quad (13)$$

Thus, the slope of $(c_v T^{3/2})$ curves versus $\frac{1}{T}$ in log scale gives good information about the energy gap. In figures 6 and 7 we have plotted $(c_v T^{3/2})$ versus $\frac{1}{T}$ for different values of the transverse field. Figure 6 shows the gap behavior close to the factorizing point, $h < h_f$, while its behavior for $h > h_f$ is presented in figure 7. A turning point of different plots in figure 7 for different transverse magnetic field is the result of different behaviors for $h < h_c \simeq 1.65$ (decreasing gap) and $h > h_c$ (linear increasing paramagnetic gap). Our results fit very well with figures 5.14 and 5.15 of [7].

Motivated by neutron-scattering results [6], Radu [7] investigated the effects of a non-commuting field on the ground state of Cs_2CoCl_4 . To be more precise in comparison, let us refer also to figure 13 of chapter 5 of [7] where the experimental data of the specific heat have been shown. The experimental data (especially in the inset of figure 13 of chapter 5 of [7]) display a double peak in the specific heat versus temperature which is for the intermediate range of magnetic field (less than the critical one).

It is also worth pointing out the behaviors of the system from the internal energy points of view. The internal energy and specific heat are related by relation $C = \frac{dU}{dT}$. The double-peak structure of the specific heat presages that, at the intermediate values of the transverse field, there are two temperatures where the internal energy of the system gets its maximum variation. In other words, at these temperatures the maximum amount of states contribute to the response functions of the systems. Thus, one can also conclude that the appearance of the two energy scales in the system is appropriate for the number of contributed states. Knowledge of these properties could be important in the study of the magneto-caloric effects of the XXZ model in the transverse field, which is a work in progress.

Acknowledgments

We would like to thank M Rezai for his helpful comments. This work was supported in part by the Center of Excellence in Complex Systems and Condensed Matter (www.cscm.ir).

References

- [1] Sachdev S 1999 *Quantum Phase Transitions* (Cambridge: Cambridge University Press)
- [2] Vojta M 2003 *Rep. Prog. Phys.* **66** 2069
- [3] Dmitriev D V, Krivnov V Ya and Ovchinnikov A A 2002 *Phys. Rev. B* **65** 172409
Dmitriev D V, Krivnov V Ya, Ovchinnikov A A and Langari A 2002 *JETP* **95** 538

- [4] Langari A 2004 *Phys. Rev. B* **69** 100402(R)
- [5] Langari A and Mahdavi S 2006 *Phys. Rev. B* **73** 54410
- [6] Kenzelmann M *et al* 2002 *Phys. Rev. B* **65** 144432
- [7] Radu T 2005 Thermodynamic characterization of heavy fermion systems and low dimensional quantum magnets near a quantum critical point *PhD Thesis* Max Planck Institute for Chemical Physics of Solids
- [8] Caux J-S, Essler F H L and Löw U 2003 *Phys. Rev. B* **68** 134431
- [9] Kurmann J, Thomas H and Muller G 1982 *Physica A* **112** 235
- [10] Roscilde T, Verrucchi P, Fubini A, Haas S and Tognetti V 2004 *Phys. Rev. Lett.* **93** 167203
- [11] Giampaolo S M, Adesso G and Illuminati F 2008 *Phys. Rev. Lett.* **100** 197201
- [12] Giampaolo S M, Adesso G and Illuminati F 2009 *Phys. Rev. B* **79** 224434
- [13] Rezaei M, Langari A and Abouie J 2010 *Phys. Rev. B* **81** 060401(R)
- [14] Aichhorn M, Daghofer M, Evertz H and von der Linden W 2003 *Phys. Rev. B* **67** 161103(R)
- [15] Siahatgar M and Langari A 2008 *Phys. Rev. B* **77** 054435
- [16] Coffman V *et al* 2000 *Phys. Rev. A* **61** 052306
- [17] Amico L *et al* 2004 *Phys. Rev. A* **69** 022304
- [18] Wootters W K 1998 *Phys. Rev. Lett.* **80** 2245